Journal of Science and Technology in Civil Engineering, NUCE 2021. 15 (1): 79–89

SIMULATION OF SEVERAL FLYING SITUATIONS OF PARAGLIDERS

Thanh Xuan Nguyen[a,*], Phuong Thi-Thu Phan[a], Tien Van Pham[a]

[a]*Faculty of Building and Industrial Construction, National University of Civil Engineering, 55 Giai Phong road, Hai Ba Trung district, Hanoi, Vietnam*

Article history:
Received 28/08/2020, Revised 23/11/2020, Accepted 03/12/2020

Abstract

Paragliding is an adventure and fascinating sport of flying paragliders. Paragliders can be launched by running from a slope or by a winch force from towing vehicles, using gravity forces as the motor for the motion of flying. This motion is governed by the gravity forces as well as time-varying aerodynamic ones which depend on the states of the motion of paraglider at each instant of time. There are few published articles considering mechanical problems of paragliders in their various flying situations. This article represents the mathematical modeling and simulation of several common flying situations of a paraglider through establishing and solving the governing differential equations in state-space. Those flying situations include the ones with constant headwind/tailwind with or without constant upwind; the ones with different scenario for the variations of headwind and tailwind combined with the upwind; the ones with varying pilot mass; and the ones whose several parameters are in the form of interval quantities. The simulations were conducted using a powerful Julia toolkit called DifferentialEquations.jl. The obtained results in each situation are discussed, and some recommendations are presented.

Keywords: paraglider; simulation; modeling; state-space; ordinary differential equations; Julia; DifferentialEquations.jl.

https://doi.org/10.31814/stce.nuce2021-15(1)-07

1. Introduction

Recently, many adventurous sports, including paragliding, have been brought to Vietnam, attracting a large number of participants. Paragliding is originally a non-motor flying sport, taking off by foot launch from a slope or by winch force from a towing vehicle. The pilot sits on a chair which is durably sewn with fabric and sturdy straps, under a wing (also called canopy) that is blown up by the air to remain aerodynamic shape and lift the paraglider up [1, 2].

There are few studies on paragliding modeling published recently. In 2008, Zaitsev and Formalskii [3] published an article on mathematical modeling and controlling a remotely controlled paraglider through an attached engine. The total velocity of the center of gravity (representing point), the angle of glide and the angle of twist of the payload were chosen to be the unknowns of the problem. Toglia and Vendittelli [4] also reported on path following for an autonomous paraglider in a input-output feedback linearizing control problem. Among the assumptions for the simplified model, the payload drag is much smaller than the canopy drag thus can be neglected. Benedetti and Pinto [5] proposed

*Corresponding author. *E-mail address:* thanhnx@nuce.edu.vn (Nguyen, T. X.)

a mechanical model for the forward motion of the paraglider where the payload drag is taken into account but the center of gravity of the whole system is assigned approximately at the harness.

A recent article of Muller et al [6] focused on the paragliding modeling and based on the book of Voight [7] on this issue. This book is written in German, dealing in detail the forces that affect to the paraglider and pilot in free flight mode without towing. By time, the aerodynamic and mechanical issues of flying objects have been more understood. In 2005, Oertel [8] clearly presented the basics of fluid mechanics as well as physical processes involved. Although these researches presented the physical phenomena and parameters affecting to a flying object, however, they did not provide a complete model particularly for the paraglider problem. In other words, according to Muller et al [6], there was no complete model for simulating the dynamic behavior and various flying situations of the paraglider system yet. Even in [6], the simulations were just for simple situations such as gliding flight where the pilot begin to fly at a certain height and a winch launch to gain altitude. This is absolutely not enough because there are many more complicated situations that may happen in an actual flight. This article develops the model of Muller et al to simulate several complex flights situations.

2. Modeling a paraglider

A rigid body diagram of forces is considered as shown in Fig. 1. The masses of the paraglider and pilot are denoted as m_d and m_p, respectively. The line connection between these two masses is assumed to be *rigid* in its axis direction. Also, paragliding flights are considered just in two dimensional plane. The right-hand-side coordinate system is used to establish the differential governing equations. The center of gravity G, defined as the point at which the sum of all the moments due to gravity is zero, is determined first. The two moments here are from the pilot weight, $W_p = m_p g$, and the gravity force of the canopy $W_d = m_d g$, as shown in Eq. (1). We next determine the distances ℓ_p and ℓ_d, where the total length of the paraglider line $\ell = \ell_p + \ell_d$ is provided by the manufacturer; and the total mass of the pilot and the canopy is $m = m_p + m_d$.

$$\left(m_p g\right)\ell_p = \left(m_d g\right)\left(\ell - \ell_p\right) \quad \text{or} \quad \ell_p = \frac{m_d \ell}{m_p + m_d} = \frac{m_d \ell}{m} \tag{1}$$

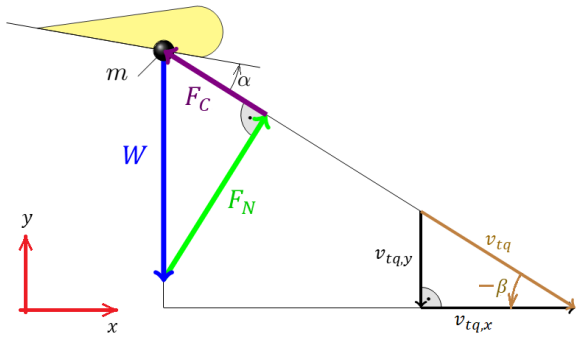

Figure 1. Relationship between the gravity force, lift force and total drag force

2.1. Velocities and aerodynamic forces

True air velocity v_{tq} with respect to the paraglider system causes the aerodynamic forces. This velocity is the relative velocity of air flow with respect to the canopy, as well as to the pilot. In a

right-hand-side coordinate system fixed at the ground, the absolute displacements of the paraglider in the direction x and y are denoted as $u_x(t)$ and $u_y(t)$, respectively. Thus, the absolute velocities of the paraglider in the direction x and y are $\dot{u}_x(t)$và $\dot{u}_y(t)$, where the dot notation over the symbol shows the time derivative. In the fixed ground coordinate system, the wind speeds in the direction x and y are denoted as v_x and v_y. The true air velocities relative to the canopy are determined as follows [9]:

$$v_{tq,x} = \dot{u}_x - v_x; \quad v_{tq,y} = \dot{u}_y - v_y \tag{2}$$

The vector sum of these air velocities is the total true air velocity and is denoted as v_{tq}. When this true air velocity is non-zero, the aerodynamic phenomena occur due to the forces caused by air flowing around the object. Typical forces with their corresponding angles of action to a paraglider under stationary conditions are shown in Fig. 1. The total gravity force W is balanced with the total aerodynamic force which is the resultant of the lift force F_N and the total drag force F_C. The total drag force is of the opposite direction of the paraglider movement. It is caused by the friction between paraglider and air, and converts a part of energy into losses. The dynamic pressure of the air acting on the paraglider is determined as $p = \rho v_{tq}^2/2$, where ρ is the air density and v_{tq} is true air velocity. The total drag force F_C is equal to the dynamic pressure p multiplied by the wing area A projected onto horizontal surface, and the drag coefficient c_c of the paraglider (Anderson [10]), as shown in Eq. (3). We have to note that the projected area A is just a reference area, we can also use frontal area or surface area of the canopy for this purpose as well, together with the corresponding drag and lift coefficients.

$$F_c = c_c A \frac{\rho}{2} v_{tq}^2 \tag{3}$$

Fig. 1 also shows that the total drag force F_C determined using a static equilibrium condition, with no inertia forces present. The total drag force can be also determined as shown in Eq. (4), where β is the angle of glide (see Fig. 1). This angle can be obtained from the true air velocity in the vertical direction and total true air velocity seen from the paraglider. Therefore, we have

$$F_C = W \sin(-\beta) = W \frac{v_{tq,y}}{v_{tq}} \tag{4}$$

From Eqs. (3) and (4), the drag coefficient can be obtained as shown in Eq. (5)

$$c_c A \frac{\rho}{2} v_{tq}^2 = W \frac{v_{tq,y}}{v_{tq}} \quad \text{and} \quad c_c = \frac{2W}{A\rho} \frac{v_{tq,y}}{v_{tq}^3} \tag{5}$$

When specifying the Eq. (4) for each component of the paragliding system, we can write the expressions of drag force acting on the canopy F_{Cd} and on the pilot F_{Cp} separately as

$$F_{Cd} = c_{Cd} A_d \frac{\rho}{2} v_{tq}^2; \quad F_{Cp} = c_{Cp} A_p \frac{\rho}{2} v_{tq}^2 \tag{6}$$

where c_{Cd} and c_{Cp} are the drag coefficients for the canopy and for the pilot, correspondingly; A_d and A_p are the areas of the canopy and the pilot, respectively.

The lift force F_N follows the same rule

$$F_N = c_N A \frac{\rho}{2} v_{tq}^2 \tag{7}$$

From Fig. 1, the lift force F_N can also be determined through the angle of glide β as shown in Eq. (8) below

$$F_N = W \cos\beta = W \frac{v_{tq,x}}{v_{tq}} \tag{8}$$

In case of the lift force, we can also implement the Eq. (7) for each component of the paragliding system (the canopy and pilot). However, the area of the pilot is much smaller than that of the canopy, thus we can ignore the lift force acting on the pilot and consider only the aerodynamic lift force acting on the canopy.

Also, from Eqs. (7) and (8), the aerodynamic lift coefficient can be obtained as follows

$$C_N A \frac{\rho}{2} v_{tq}^2 = W \frac{v_{tq,x}}{v_{tq}} \quad \text{or} \quad c_N = \frac{2W}{A\rho} \frac{v_{tq,x}}{v_{tq}^3} \tag{9}$$

Based on the Eqs. (5) and (9), there have been many experiments to measure the aerodynamic drag coefficient c_c and aerodynamic lift coefficient c_N corresponding to different types of paragliders and angles of glide. In the simulations of flight situations shown in Section 3, these coefficients are taken from [6].

2.2. *Angles and distances*

From the geometric relationship shown in Fig. 2, the angle of glide β is determined by

$$\beta = \text{atan}\left(\frac{v_{tq,y}}{v_{tq,x}}\right) \tag{10}$$

The angle of attack α is the angle at which the air meets the canopy (Currer [9]). In Fig. 2, this angle is defined between the chord line and the flight direction. It affects the pendulum moment about the pitch axis and can be controlled by the pilot via the brake lines.

The angle of twist φ is the angle between the horizontal line and the chord line. It is also the angle between the vertical line and the suspension line to the pilot. As in Fig. 2, we have

$$\alpha = \varphi - \beta \tag{11}$$

From Fig. 3 and previously shown relationships, the distances ℓ_1 to ℓ_5 (lever arms – the distances from the center of gravity to the forces $W_p, W_d, F_{Cp}, F_{Cd}, F_N$, respectively) in Fig. 3 can be obtained as follows

$$\ell_1 = \ell_p \sin(-\varphi)\,; \ell_2 = \ell_d \sin(-\varphi) \tag{12a}$$

$$\ell_3 = \ell_p \cos\alpha; \ell_4 = \ell_d \cos\alpha; \ell_5 = \ell_d \sin\alpha \tag{12b}$$

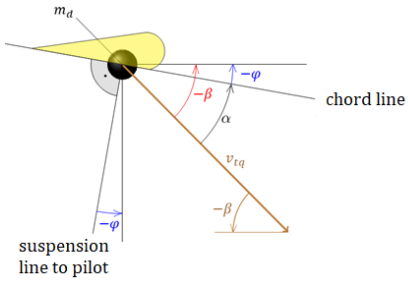

Figure 2. The angles

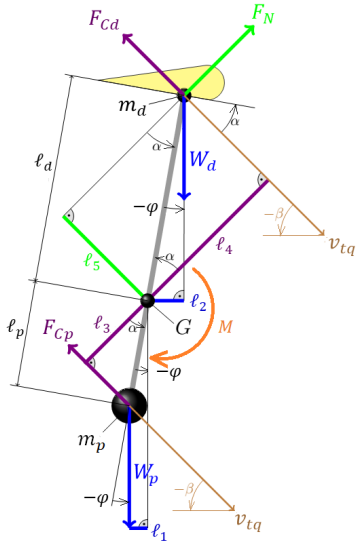

Figure 3. Forces acting on the paraglider system

2.3. *Equations of motion*

The absolute acceleration in the direction x and y are $\ddot{u}_x(t)$ and $\ddot{u}_y(t)$, respectively. The inertia force in x direction is the product of total mass m and absolute acceleration in x direction $\ddot{u}_x(t)$. The inertia force in y direction is determined similarly. For the free body diagram of forces acting on the paraglider as shown in Fig. 3, by adapting the principle of D'Alembert, the sum of all forces acting on the whole system, including inertia forces in x axis, should vanish

$$m\ddot{u}_x(t) = -F_{Cd}\cos(-\beta) - F_{Cp}\cos(-\beta) + F_N\sin(-\beta) \tag{13a}$$

Similarly, also by the principle of D'Alembert, we have below equation for forces along y axis, with the same rule.

$$m\ddot{u}_y(t) = -W_p - W_d + F_{Cd}\sin(-\beta) + F_{Cp}\sin(-\beta) + F_N\cos(-\beta) \tag{13b}$$

The sum of all moments about the center of gravity G is zero with the lever arms from ℓ_1 to ℓ_5 as obtained in Section 2.2. The angular velocity and angular acceleration of the system are denoted as $\dot{\varphi}$ and $\ddot{\varphi}$. The sum of all torques about the gravity point G equals to the moment of rotational inertia J multiplied by the angular acceleration

$$J\ddot{\varphi} = W_p\ell_1 - W_d\ell_2 - F_{Cp}\ell_3 + F_{Cd}\ell_4 - F_N\ell_5 - M \tag{13c}$$

where the moment of rotational inertia J about the pivot axis going through the point G is

$$J = m_d\ell_d^2 + m_p\ell_p^2 \tag{14}$$

The damping torque M caused by the movement of the air is calculated by the product of the viscous damping coefficient in the rotational motion c and the corresponding angular velocity

$$M = c\dot{\varphi} \tag{15}$$

2.4. System modeling in state space

The state variables are defined as follows

$$\mathbf{Z} = \begin{bmatrix} u_x & \dot{u}_x & u_y & \dot{u}_y & \varphi & \dot{\varphi} \end{bmatrix}^T = \begin{bmatrix} z_1 & z_2 & z_3 & z_4 & z_5 & z_6 \end{bmatrix}^T \tag{16}$$

Then, Eqs. (13) can now be reformed in state space as

$$\dot{\mathbf{Z}} = f(Z,t) \tag{17}$$

where $f = \begin{bmatrix} f_1 & f_2 & f_3 & f_4 & f_5 & f_6 \end{bmatrix}^T$ are defined as:

$$f_1 = z_2 \tag{18a}$$

$$f_2 = \frac{1}{m}\left(-F_{Cd}\cos(-\beta) - F_{Cp}\cos(-\beta) + F_N\sin(-\beta)\right) \tag{18b}$$

$$f_3 = z_4 \tag{18c}$$

$$f_4 = \frac{1}{m}\left(-W_p - W_d + F_{Cd}\sin(-\beta) + F_{Cp}\sin(-\beta) + F_N\cos(-\beta)\right) \tag{18d}$$

$$f_5 = z_6 \tag{18e}$$

$$f_6 = \frac{1}{J}\left(W_p\ell_1 - W_d\ell_2 - F_{Cp}\ell_3 + F_{Cd}\ell_4 - F_N\ell_5 - cz_6\right) \tag{18f}$$

Based on Eqs. (16) to (18) above, four different flight situations are considered as follows.

- Situation 1: the input to the model of paraglider includes the constant wind speeds in both horizontal and vertical directions (v_x is positive for the headwind and negative for tailwind; v_y is positive for upwind and negative for downwind).

- Situation 2: the input to the model of paraglider are time-varying wind speeds following some arbitrary functions $v_x = v_x(t)$ and $v_y = v_y(t)$.

- Situation 3: the mass reduction of the payload (pilot and the harness) during a certain of time interval is considered. This is a practical situation where the pilot in a paragliding process can reduce the additional payload (contained in a water tank in the harness) to achieve a desired flying performance. In this case, the total mass of the pilot and the harness can be modeled as a decreasing function $m_p = m_p(t)$. Other related quantities such as center of gravity G, or moment of rotational inertia J, will then be calculated correspondingly.

- Situation 4 is also another common situation in practice where the mass of payload is not a certain known value. Instead, we just know that it is in a certain interval, such as from 60 kg to 90 kg. In this case, the mass of the payload is modeled as a interval quantity $m_p = \left[\underline{m_p}; \overline{m_p}\right]$ with the lower bound and upper bound are $\underline{m_p}$ and $\overline{m_p}$, respectively.

3. Simulating the flight situations

3.1. Simulation tool

In this article, the tool to simulate the flying situations of a paraglider is DifferentialEquations.jl package, written in Julia language. Julia is a free and open source software, with fast processing speed for many basic as well as advanced computing tasks [11]. The DifferentialEquations.jl tool is a package of subroutines written in Julia, which help solve differential equations fast and efficiently. The typical equations that this package can solve are very diverse, including: discrete equations, ordinary differential equations (ODE), split and partitioned ODEs, stochastic ODEs, differential algebraic equations (DAE), delay differential equations, mixed discrete and continuous equations. This tool is optimized to solve differential equations in the fastest and most efficient way, using classical and modern algorithms, featuring classic methods written in C/Fortran languages. All algorithms are thoroughly tested to ensure the accuracy via convergent tests [12].

3.2. Simulation parameters

The important parameters used in simulations are from [6] or theoretically calculated. The viscous damping coefficient c in rotational motion is taken at 10^4 Nms/rad to reflect the reality. The aerodynamic drag coefficient for pilot is equal to 0.33 [6].

$$\begin{array}{cccc} \rho = 1.27\ \text{kg/m}^3 & A_p = 1.0\ \text{m}^2 & m_d = 6\ \text{kg} & \ell_p = 0.395\ \text{m} \\ m_p = 90\ \text{kg} & \ell_d = 6.575\ \text{m} & \ell = 6.97\ \text{m} & A_d = 24.26\ \text{m}^2 \end{array}$$

The drag coefficient c_{Cd} and aerodynamic lift coefficient c_N are function of the angle of attack α. From experimental data [13], this dependence can be approximated by following functions

$$c_N(\alpha) = \frac{2\alpha + 11}{300}, \qquad c_{Cd}(\alpha) = \frac{65\alpha + 70}{1000} \tag{19}$$

3.3. Simulation results

a. Situation 1

This simulation is served as a check of our coding for the simulation. The starting height is 500 m and launching speed of pilot is 2 m/s, while speed of the headwind or tailwind in consideration is

3 m/s, time of survey is 60 seconds. This situation is also expanded to include an additional upwind at a velocity of 0.5 m/s. The results are shown in Figs. 4 and 5. The travelling distances, flying vertical level (altitude) and twist angle obtained from the simulations are similar to those in [6]. We say "similarity" since they share almost the same variation with time. The exact comparison could not be done since there is no particular wind speed given explicitly in [6] when they conducted the simulation.

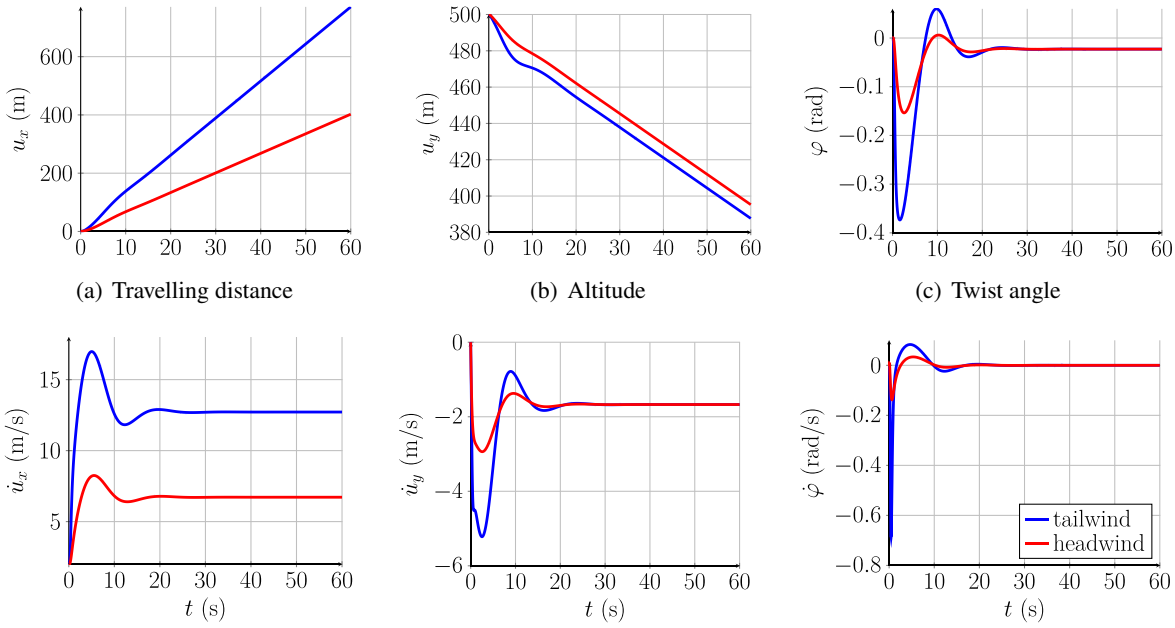

(a) Travelling distance (b) Altitude (c) Twist angle

(d) Horizontal velocity (e) Vertical velocity (f) Angular velocity

Figure 4. Flying with headwind and tailwind

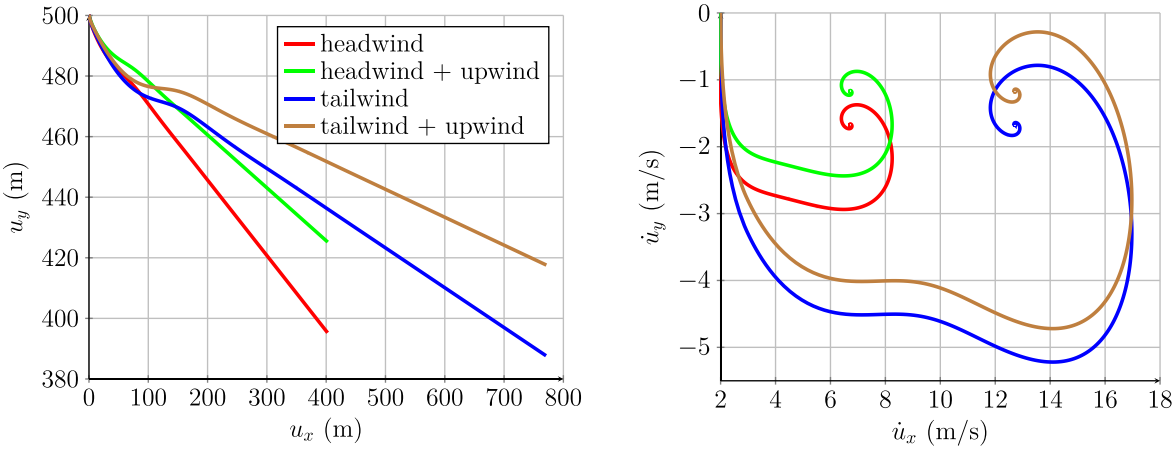

(a) $u_x(t)$ *vs.* $u_y(t)$ (b) $\dot{u}_x(t)$ *vs.* $\dot{u}_y(t)$

Figure 5. Flying with headwind and tailwind, in addition with upwind

It can be seen from Fig. 5 that the travelling horizontal distances with the headwind and the tailwind are almost linear over time, but the difference between the two cases is large. Meanwhile, the altitude and twist angle are just slightly different in these two cases. We have the same comment for the velocities along the two axes and for the angular velocity. The addition of upwind, even with a low velocity, creates a significant difference in the relation of distances as well as the velocities of the paraglider in both directions as shown in Fig. 5.

b. Situation 2

The starting height is 500 m and launching speed of pilot is 2 m/s. Consider the flight in two cases that follow. In the first case, the constant headwind velocity is 3 m/s during 10 seconds without upwind, then during the next 20 seconds, the headwind velocity decreases linearly to minus 3 m/s to be tailwind. Also during this interval of time, there occurs upwind with the increasing velocity from 0 m/s at the instant of time 10 seconds to 1.2 m/s at the instant of time 30 seconds. After that time interval, the wind velocities become constants again. In the second case, the scenario is similar but the tailwind of velocity 3 m/s is considered first, and it continually and linearly changes to be headwind, also of the velocity 3 m/s. The results from these two cases are shown in Fig. 6.

These results show that the lost in altitude in both cases is approximately the same. However, the paraglider travels a bit longer distance in Case 1 than in Case 2. The variation of horizontal and vertical velocities of the paraglider clearly reflect the variation the wind velocities, with a certain delay. In some first seconds, there are always large variations in velocities of paraglider in both directions. Fig. 6(a), as well as Fig. 5(a) in Situation 1 show the minimum slope of the paraglider launching field for taking off is about 1 : 4.

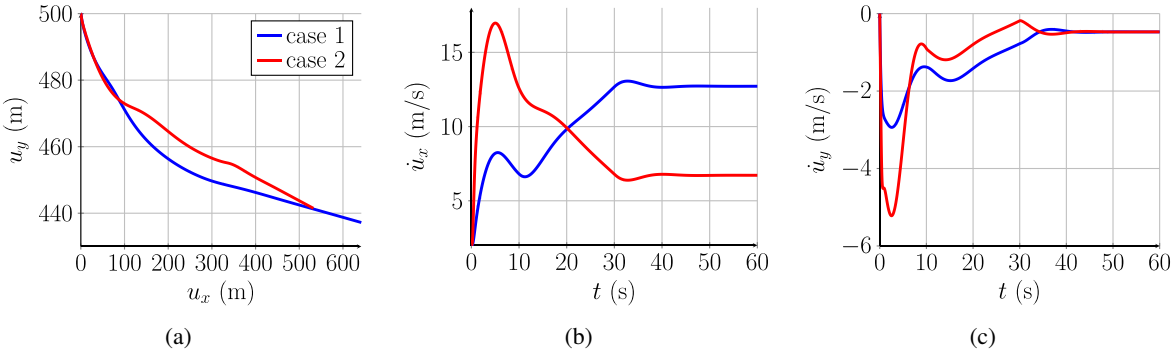

Figure 6. (a) relation between traveling distance and the altitude; (b) horizontal velocity as a function of time; (c) vertical velocity as a function of time

c. Situation 3

The starting height is 500 m, pilot's launching speed is 2 m/s, the headwind speed is 3 m/s, upwind speed is 1.5 m/s. The reduction in payload mass is given as below:

$$m_p(t) = \begin{cases} 90, & t \le 10 \\ 90 - 0.4\,(t-10), & 10 \le t \le 30 \\ 82, & t \ge 30 \end{cases} \tag{20}$$

The simulation results of this situation (shown in red line), compared to the normal flight with no mass reduction (shown in blue line) are shown in Fig. 7. Normally, the mass withdrawal of about 8 kg

(of water) does not affect much the absolute velocities of the paraglider. However, the altitude loss decreases due to the loss of payload. The traveling distance also decreases, but of less amount. These results are in accordance with actual observations.

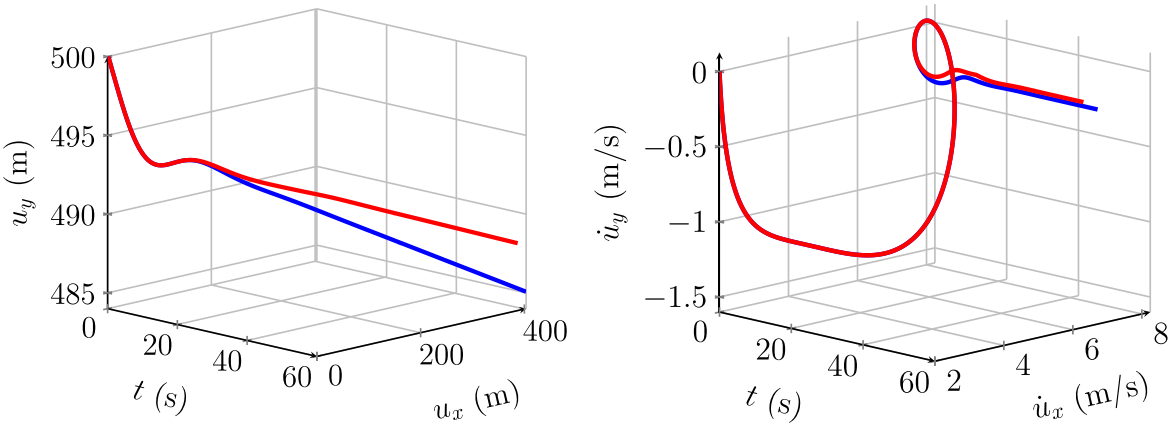

(a) Distances in both directions with respect to time

(b) Velocities in both directions with respect to time

Figure 7. Comparison of flight in two cases

d. Situation 4

The mass of payload is an uncertain quantity. Assume that the mass is some value in the range of from 60 kg to 90 kg, and is modeled as an interval variable $m_p = 75 \pm 15$. Similarly, the viscous damping coefficient c is modeled as another interval quantity $c = 10^4 \pm 3000$. Other input parameters are given as: the starting height is 500 m, pilot's launching speed is 2 m/s, the headwind speed is 3 m/s, and there is no upwind. Using the tool in Julia language tailored for manipulating interval quantities, the simulation results in the first 20 seconds are received as shown in Fig. 8.

Each state variable was computed with the lower bound and upper bound. The the uncertainty of the each state variable can be shown through the width of the obtained interval. For the traveling distances along x- and y-axis, the interval's width increase over time. This interval's width for twist angle is quite large at the beginning then getting smaller when the flight gets into steady state mode. This is a rather strange result, possibly due to the limitations in mathematical operations on interval quantities. This observation is also shown in the subfigures for velocities. From these results, the landing area of the paraglider can be estimated, also in the interval values.

In case the parameters are not deterministic, we can also model with noise scaling factor σ and then use Monte-Carlo simulations. For instance, in the above situation, with $\sigma = 0.2$ at each time step, the obtained results can be illustrated in Fig. 9 (for clarity of the plots, the results are shown for only 30 samples in the first 20 seconds). We can see that the uncertainty in the output increases over time. Through the results shown in Fig. 8 and Fig. 9, it can be seen that limitations in mathematical operations with interval quantities are removed when using Monte-Carlo simulations, no strange results as shown in Fig. 8(c) to 8(f) anymore.

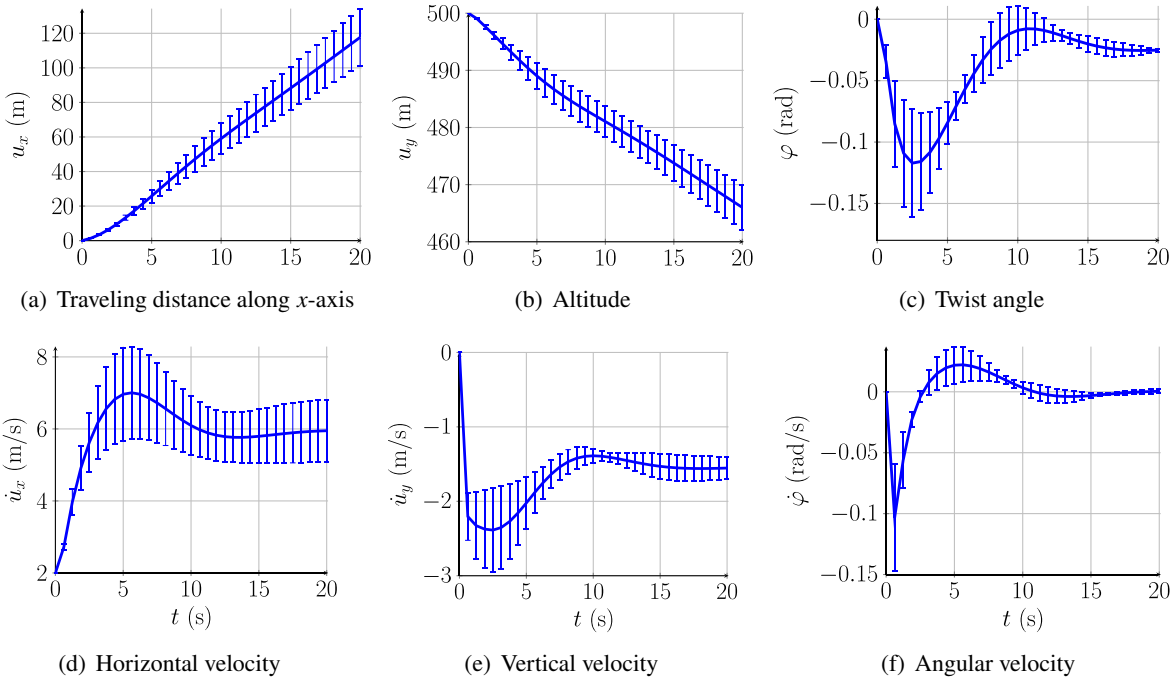

(a) Traveling distance along x-axis (b) Altitude (c) Twist angle

(d) Horizontal velocity (e) Vertical velocity (f) Angular velocity

Figure 8. Interval values

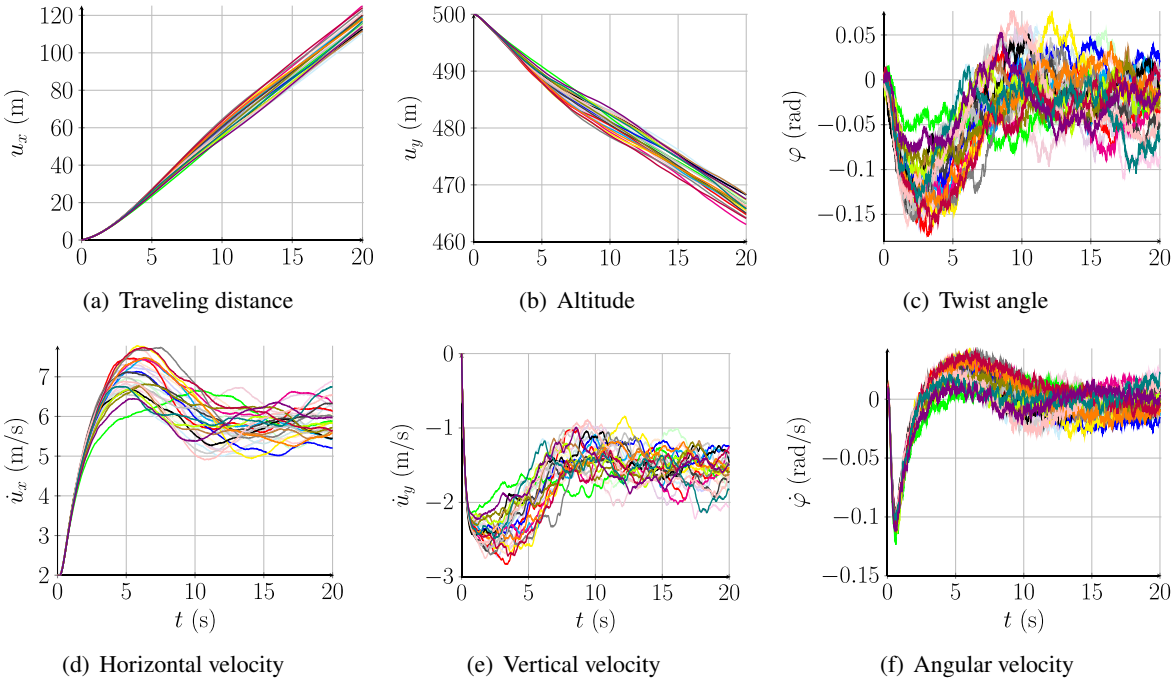

(a) Traveling distance (b) Altitude (c) Twist angle

(d) Horizontal velocity (e) Vertical velocity (f) Angular velocity

Figure 9. Some of Monte-Carlo simulations

4. Conclusion and suggestion

Some actual flight situations of paraglider are modeled and simulated by establishing the motion equations in 2D state space with two variables of translational displacements (traveling distances in horizontal and vertical axes) and one rotational displacement (twist angle). The received system of differential equations is nonlinear each of which is uncoupled in terms of unknowns. The simulation was carried out by the effective tool, called DifferentialEquations.jl, for solving differential equations written in Julia open programing language. The simulation results are consistent with the observations that allow us to gain a deeper understanding of the dynamics of the paragliding system and allow us to predict the states of the system, helping pilots to control the paraglider more flexibly and accurately. To our best knowledge, these are new results that have never been published elsewhere before. The research can be developed for the problem in 3D space, or for the problem of paragliding under the control of pilots or towing vehicles.

References

[1] Wikipedia. *Paragliding*. Accessed 07/29/2020.
[2] Pagen, D. (2001). *The art of paragliding*. Black Mountain Books.
[3] Zaitsev, P. V., Formal'skii, A. M. (2008). Paraglider: Mathematical model and control. *Doklady Mathematics*, 77(3):472–475.
[4] Toglia, C., Vendittelli, M., Lanari, L. (2010). Path following for an autonomous paraglider. In *49th IEEE Conference on Decision and Control (CDC)*, IEEE, 4869–4874.
[5] Benedetti, D. M., de Freitas Pinto, R. L. U. (2007). A paraglider longitudinal flight mechanics modeling. Technical report, Society of Automotive Engineers Transaction (No. 2007-01-2952).
[6] Müller, M., Ali, A., Tareilus, A. (2018). Modelling and simulation of a paraglider flight. In *Proceedings of The 9th EUROSIM Congress on Modelling and Simulation, EUROSIM 2016 and The 57th SIMS Conference on Simulation and Modelling SIMS 2016*, number 142, Linköping University Electronic Press, 327–333.
[7] Voigt, O. (2003). *Aerodynamik und Flugmechanik des Gleitschirms*. Norderstedt: Schweiz.
[8] Oertel, H. (2005). *Introduction to Fluid Mechanics: Fundamentals and Applications*. Karlsruhe: Universitatsverlag.
[9] Currer, I. (2011). *Touching Cloudbase - The Complete Guide to Paragliding*. New York: Air Supplies.
[10] Anderson, J. (2005). *Introduction to Flight*. New York: McGraw-Hill.
[11] The Julia Language. *A fresh approach to technical computing*. Accessed 07/29/2020.
[12] *DifferentialEquations.jl Documentation*. Accessed 07/29/2020.
[13] *Skywalk - Paragliders*. Accessed 07/29/2020.